

University of Nebraska - Lincoln

DigitalCommons@University of Nebraska - Lincoln

Biochemistry -- Faculty Publications

Biochemistry, Department of

6-21-2023

Type IV Pilus-Mediated Inhibition of *Acinetobacter baumannii* Biofilm Formation by Phenothiazine Compounds

Nam Vo

Benjamin S. Sidner

Yafan Yu

Kurt H. Piepenbrink

Follow this and additional works at: <https://digitalcommons.unl.edu/biochemfacpub>



Part of the [Biochemistry Commons](#), [Biotechnology Commons](#), and the [Other Biochemistry, Biophysics, and Structural Biology Commons](#)

This Article is brought to you for free and open access by the Biochemistry, Department of at DigitalCommons@University of Nebraska - Lincoln. It has been accepted for inclusion in Biochemistry -- Faculty Publications by an authorized administrator of DigitalCommons@University of Nebraska - Lincoln.



Type IV Pilus-Mediated Inhibition of *Acinetobacter baumannii* Biofilm Formation by Phenothiazine Compounds

Nam Vo,^a Benjamin S. Sidner,^a Yafan Yu,^{a,b}  Kurt H. Piepenbrink^{a,b,c,d,e}

^aDepartment of Biochemistry, University of Nebraska-Lincoln, Lincoln, Nebraska, USA

^bDepartment of Food Science and Technology, University of Nebraska-Lincoln, Lincoln, Nebraska, USA

^cDepartment of Chemistry, University of Nebraska-Lincoln, Lincoln, Nebraska, USA

^dNebraska Food for Health Center, University of Nebraska-Lincoln, Lincoln, Nebraska, USA

^eCenter for Integrated Biomolecular Communication, University of Nebraska-Lincoln, Lincoln, Nebraska, USA

ABSTRACT Infections by pathogenic *Acinetobacter* species represent a significant burden on the health care system, despite their relative rarity, due to the difficulty of treating infections through oral antibiotics. Multidrug resistance is commonly observed in clinical *Acinetobacter* infections and multiple molecular mechanisms have been identified for this resistance, including multidrug efflux pumps, carbapenemase enzymes, and the formation of bacterial biofilm in persistent infections. Phenothiazine compounds have been identified as a potential inhibitor of type IV pilus production in multiple Gram-negative bacterial species. Here, we report the ability of two phenothiazines to inhibit type IV pilus-dependent surface (twitching) motility and biofilm formation in multiple *Acinetobacter* species. Biofilm formation was inhibited in both static and continuous flow models at micromolar concentrations without significant cytotoxicity, suggesting that type IV pilus biogenesis was the primary molecular target for these compounds. These results suggest that phenothiazines may be useful lead compounds for the development of biofilm dispersal agents against Gram-negative bacterial infections.

IMPORTANCE *Acinetobacter* infections are a growing burden on health care systems worldwide due to increasing antimicrobial resistance through multiple mechanisms. Biofilm formation is an established mechanism of antimicrobial resistance, and its inhibition has the potential to potentiate the use of existing drugs against pathogenic *Acinetobacter*. Additionally, as discussed in the manuscript, anti-biofilm activity by phenothiazines has the potential to help to explain their known activity against other bacteria, including *Staphylococcus aureus* and *Mycobacterium tuberculosis*.

KEYWORDS *Acinetobacter*, biofilm, phenothiazine, thioridazine, type IV pili

A *Acinetobacter* species are nonflagellated, Gram-negative coccobacilli which can be found in a wide range of terrestrial or aquatic environments but also form commensal or pathogenic relationships with human hosts. *Acinetobacter baumannii*, in particular, is known to cause infections in the lungs, skin, urinary tract, and blood, and many infections are also caused by the closely related *A. calcoaceticus*, *A. nosocomialis*, and *A. pittii* (the *Acinetobacter calcoaceticus-baumannii* or Acb complex) (1). The CDC 2019 antibiotic resistance threat report classifies carbapenem-resistant *Acinetobacter* (CARB), regardless of species, as an urgent threat because of the difficulty of treating these multidrug-resistant infections (2). Because of its multidrug resistance, *A. baumannii* is also included in the list of ESKAPE pathogens (*Enterococcus faecium*, *Staphylococcus aureus*, *Klebsiella pneumoniae*, *Acinetobacter baumannii*, *Pseudomonas aeruginosa*, and *Enterobacter* spp.) (3). Much like another ESKAPE pathogen, *P. aeruginosa*, most *Acinetobacter* infections are nosocomial, being most commonly associated with the use of ventilators or catheters (4).

Editor John M. Atack, Griffith University

Copyright © 2023 Vo et al. This is an open-access article distributed under the terms of the [Creative Commons Attribution 4.0 International license](https://creativecommons.org/licenses/by/4.0/).

Address correspondence to Kurt H. Piepenbrink, kurt.piepenbrink@unl.edu.

The authors declare no conflict of interest.

Received 7 March 2023

Accepted 26 May 2023

Published 21 June 2023

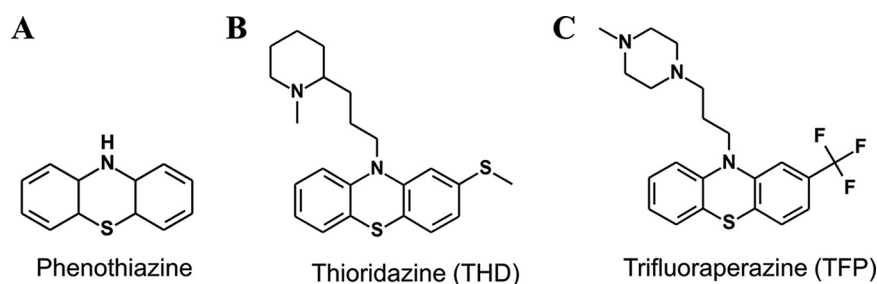


FIG 1 Phenothiazine compounds. Chemical structures of (A) phenothiazine and two derivatives, (B) thioridazine (THD) and (C) trifluoperazine (TFP).

One critical factor in the epidemiology of *Acinetobacter* infections and the difficulty of treating them is the ability of *Acinetobacter* to form biofilms on biotic (host tissue) and abiotic (metal or plastic) surfaces. Biofilms formed on medical devices can be a source of transmission from patient to patient, and biofilms allow for both persistent and recurrent infections in health care settings. Bacterial biofilms are multicellular structures composed of bacterial cells encased in an extracellular matrix of polypeptides, polysaccharides, and DNA. Bacterial biofilms form an encapsulating barrier against host or environmental factors, making cells within a biofilm more resistant to antibiotic compounds than planktonic cells.

Bacterial biofilm formation is a multi-factorial process with numerous secreted proteins (5), extracellular appendages (6–9), and quorum-sensing mechanisms (10) implicated in various species. In *Acinetobacter*, our group previously found that type IV pili are essential for robust biofilm formation in vertical biofilm assays (11). Type IV pili (T4P) are helical filaments comprised of protein subunits (pilins) stabilized by the association of hydrophobic N-terminal alpha helices in the core of the pilus fiber (12, 13). They can be extended or retracted through complex membrane-spanning machinery, allowing them to function in adhesion, DNA uptake (14, 15), and surface motility (16) in numerous Gram-negative and Gram-positive species. Twitching motility, a form of surface motility which can occur at the interface between solid and semisolid surfaces, is mediated solely by T4P (17–20) and requires both efficient extension and retraction of the pilus (16, 21, 22). T4P are well-characterized in *Neisseria*, where they are essential for the formation of microcolonies on host cells (23, 24). To inhibit host adhesion by *Neisseria*, Denis et al. screened for inhibitory compounds and found two structurally related compounds which acted specifically through the inhibition of T4P in *Neisseria meningitidis* (25). These two compounds, trifluoperazine (TFP) and thioridazine (THD), belong to the family of phenothiazine derivatives or phenothiazines (Fig. 1).

Phenothiazines are a class of heterocyclic compounds with a variety of applications and a widespread history of use in biology and medicine. Derivatives of phenothiazine have been used as histological stains (26), sedatives (27), antipsychotic agents (28), and antimicrobials (29, 30). One piperidine, thioridazine, has been shown to have activity against both extensively drug-resistant *Mycobacterium tuberculosis* (31, 32) and methicillin-resistant *S. aureus* (MRSA) (33–35). For both of these organisms, the primary therapeutic effect has been the potentiation of other antimicrobial compounds due to diminished capacity for microbial resistance.

The phenothiazine compounds previously found to inhibit *Neisseria* microcolony formation were also found to inhibit T4P-dependent functions in *P. aeruginosa* in the same study, suggesting that they may have broad activity against Gram-negative T4P systems, including those in *Acinetobacter*. Here, we report the activity of phenothiazine compounds against T4P-dependent functions, including biofilm formation, in *A. baumannii* and other *Acinetobacter* species.

RESULTS

Thioridazine and trifluoperazine are well-tolerated by *A. baumannii* and *P. aeruginosa*, but not by *Moraxella bovoculi*, at μM concentrations. To gauge the suitability of phenothiazines as inhibitors of type IV pilus production in *Acinetobacter* and related genera, we

first used planktonic growth in the presence of working concentrations of two phenothiazines to measure bacteriostatic or bacteriotoxic activity. For species where these compounds are cytotoxic, inhibition of specific functions (twitching motility or biofilm formation) might be difficult to disentangle from cytotoxicity. Previous studies of phenothiazines as antimicrobials against *S. aureus*, *N. meningitidis*, and *M. tuberculosis* used concentrations ranging from 2 to 120 μM , with MIC values as low as 20 μM depending on the species in question (25, 32, 35). Most recently, to inhibit T4P function in *Neisseria*, Denis et al. (25) used concentrations of two phenothiazine-derivatives, thioridazine and trifluoperazine (Fig. 1), at concentrations ranging from 10 to 40 μM , observing effects on T4P function in as little as 30 min and growth defects after approximately 2 h.

To compare the bactericidal or bacteriostatic activity of THD and TFP against *Acinetobacter* to these previous observations, we chose concentrations of 10 and 50 μM , encompassing the range where both inhibition of T4P function and potentiation of other antimicrobials were observed. We measured the growth in broth of three *Pseudomonadales* species, *Acinetobacter nosocomialis* M2, *P. aeruginosa* PAO1, and *Moraxella bovoculi* 58086, at 10 and 50 μM THD, as well as *A. nosocomialis* and *M. bovoculi* at 10 and 50 μM TFP. Over 12 h, *A. nosocomialis* and *P. aeruginosa* showed nearly identical optical density of bacterial cultures at 0, 10, and 50 μM THD. *A. nosocomialis* also showed no substantial growth defect at 10 or 50 μM TFP over the observed time course (6 h). However, both compounds significantly limited the growth of *M. bovoculi* at 10 μM . For each curve (Fig. S1 in the supplemental material), bacteria in 96-well plates were incubated at 37°C, shaken every 30 minutes, and optical density was measured immediately afterward. Due to the cytotoxicity of TFP and THD against *M. bovoculi*, further investigations used *Acinetobacter* and *Pseudomonas* species.

Phenothiazines inhibit twitching motility in *Acinetobacter*. To measure the effects of phenothiazines on T4P activity, we used a twitching motility assay. Twitching motility is surface-based, first observed in *A. calcoaceticus* (19–21), and can occur on semisolid surfaces or at the interface of solid and semisolid surfaces. Unlike in some other forms of surface motility, T4P is essential for twitching motility, which requires both T4P biogenesis and retraction, allowing it to be used as a proxy for T4P biogenesis and function. Fig. 2 shows twitching assays for *A. nosocomialis* wild type, ΔpilA (knockout of the major pilus subunit, unable to produce type IV pili), and a chromosomal complement (Fig. 2A) *A. nosocomialis* twitching at 0, 10, and 50 μM THD (Fig. 2B and C), as well as comparisons of *A. nosocomialis*, *A. baumannii*, and *P. aeruginosa* twitching with the addition of either TFP or THD at 50 μM (Fig. 2D to F). As described in Materials and Methods, twitching was measured at the interface between low-percentage MacConkey agar (1%) and the solid plastic surface of the petri dish. While results were similar for both compounds against *P. aeruginosa* and *A. baumannii*, only THD showed a statistically significant effect against *A. nosocomialis*; this effect was dose-dependent, with a significant ($P = 0.0025$) reduction at 50 μM , but not at 10 μM .

The precise mechanism of this inhibition remains unclear. Denis et al. hypothesized that phenothiazines inhibit microcolony formation in *Neisseria* by disrupting sodium transport across the inner membrane and showed that increasing NaCl concentrations can counteract the dispersal effect (25). However, microcolony formation in *Neisseria* appears to be largely independent of NaCl concentration. Based on prior results from other studies, we hypothesized that in *Acinetobacter* species, T4P function would decrease with increasing salinity (36). Figure S2 shows the effects of increasing salinity on T4P function in *A. baumannii* and *P. aeruginosa*; this assay is identical to that shown in Fig. 2, with NaCl added to the MacConkey agar medium at final concentrations of 100 and 200 mM. While no significant differences were observed between the three NaCl concentrations for *P. aeruginosa*, *A. nosocomialis* showed a clear optimum at 100 mM NaCl, with a significant reduction in twitching at 200 mM. The dependence of *Acinetobacter* T4P activity upon salinity implies that sodium transport is insufficient to promote T4P biogenesis and that other inhibitory mechanisms are upregulated at higher NaCl concentrations.

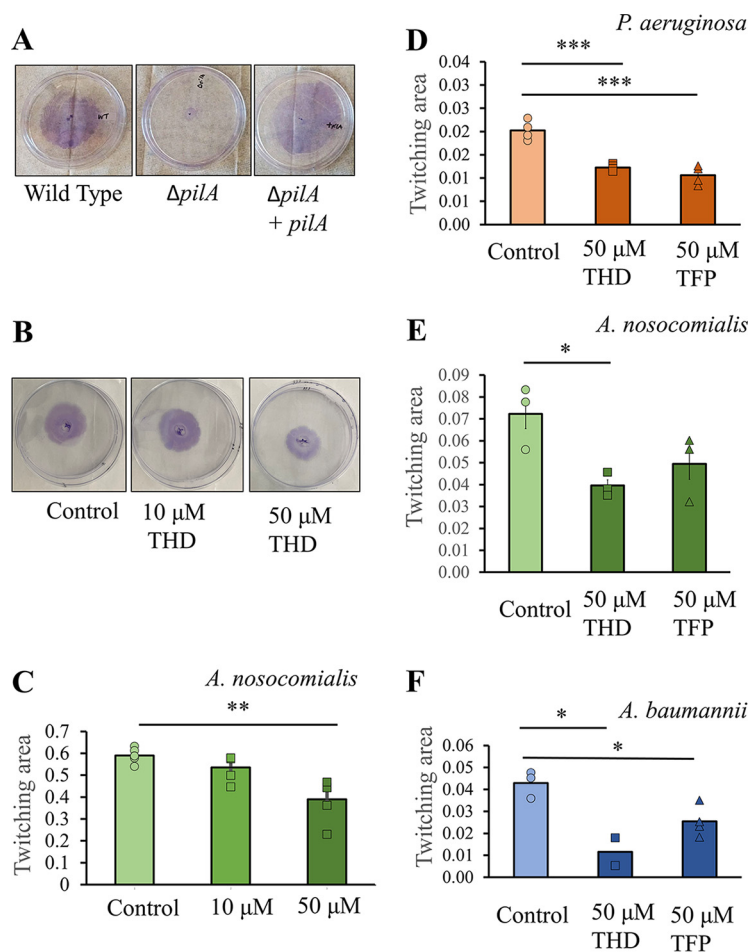


FIG 2 Twitching motility. (A) Representative twitching from plates inoculated with *A. nosocomialis* M2 wild type, $\Delta pilA$, and $\Delta pilA$ complemented chromosomally with *pilA*. (B) Representative twitching from *A. nosocomialis* M2; control plates and those with 10 and 50 μ M thioridazine. (C) Twitching area as a function of THD concentration. (D to F) Comparisons of twitching inhibition from THD (squares) and TFP (triangles) are shown for (D) *P. aeruginosa* PAO1, (E) *A. nosocomialis* M2, and (F) *A. baumannii* ATCC 17978. *, $P < 0.05$; **, $P < 0.01$; ***, $P < 0.001$.

Static biofilm formation assays show reduced biofilm formation for *Acinetobacter* and *Pseudomonas* treated with phenothiazines. Previously, our group showed that *Acinetobacter* mutant strains lacking type IV pili were deficient in static assays of biofilm formation (11). Similar results have been shown in *P. aeruginosa* for T4P-deficient mutants (37, 38), and hyperpiliated mutants of *P. aeruginosa* show increased biofilm formation (39). Denis et al. also showed dispersal of *P. aeruginosa* biofilms at 100 μ M TFP (25). Based on this established relationship and the results described above, we hypothesized that phenothiazine treatment would similarly inhibit biofilm formation by *Acinetobacter*.

Figure 3A shows the results of static biofilm assays for *A. nosocomialis* M2 and *A. baumannii* ATCC 17978 with the addition of 50 μ M THD or TFP. As described in Materials and Methods, these biofilms were grown in plates with minimal shaking at 37°C and the planktonic cells were removed, washed, and stained with crystal violet (40). At this concentration, both compounds significantly reduced biofilm formation in *A. baumannii*; however, in *A. nosocomialis*, only the TFP result was statistically significant, reversing the trend seen for *A. nosocomialis* twitching motility. Titrations of THD showed a dose-dependent effect in *A. baumannii* (Fig. 3D), but only the 50- μ M concentration was effective against *P. aeruginosa* PAO1 and *A. nosocomialis* M2 (Fig. 3C and D). Taken together, these results support an inhibitory effect for phenothiazines, particularly thioridazine, on *Acinetobacter* biofilm formation, with more consistent inhibition seen for *A. baumannii* ATCC 17978 (a historical lab strain) than

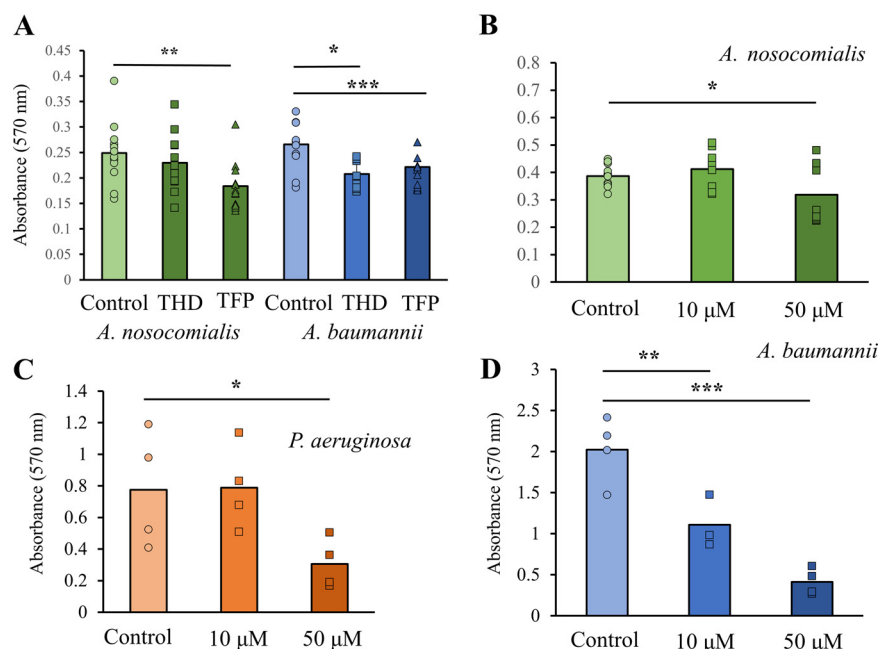


FIG 3 Static biofilm formation. (A) Static biofilm assay showing the effects of 50 μ M TFP (triangles) and THD (squares) for *A. nosocomialis* M2 and *A. baumannii* 17978. (B to D) Static biofilm formation as a function of THD concentration is shown for (B) *A. nosocomialis* M2, (C) *P. aeruginosa* PAO1, and (D) *A. baumannii* 17978. *, $P < 0.05$; **, $P < 0.01$; ***, $P < 0.001$.

for *A. nosocomialis* M2 (a more recent isolate). However, the high level of variability makes it difficult to gauge the species-specificity of each compound.

Because polysaccharides make up a portion of the extracellular matrix of bacterial biofilms (9), the formation of bacterial biofilm can result in the selective uptake of dyes which adhere to polysaccharides. Assays of Congo red uptake have been used as a measure of biofilm formation in *P. aeruginosa* (41). We measured the uptake of Congo red by several *Acinetobacter* species, with and without the addition of THD, and did not find significant effects for any species or strain of *Acinetobacter* despite considerable natural variation between species (Fig. S3). The insensitivity of this assay to phenothiazine compounds could indicate that biofilm formation and polysaccharide production are less correlated in *Acinetobacter* species than in *P. aeruginosa* or that biofilm formation on agar medium is less dependent upon T4P function.

Continuous flow model of biofilm formation shows that T4P-mutants of *A. nosocomialis* are deficient in biofilm formation. To evaluate the effect of phenothiazines on a more robust assay of *Acinetobacter* biofilm formation, we used a continuous flow assay in which biofilms develop under continuous shear stress (42). As an initial test of the system and to ensure that *Acinetobacter* biofilm formation under continuous flow was equally dependent on T4P, we measured biofilm formation for *A. nosocomialis* M2 wild type, $\Delta pilA$, and $\Delta pilA + ppilA$: the wild-type strain, a knockout strain of the major pilin subunit, and its complement (11, 16, 43). These results, shown in Fig. S4, show a clear defect in the $\Delta pilA$ mutant which is restored in the complement.

Figure 4 shows the results of continuous flow biofilm formation for *A. nosocomialis* with the addition of THD at 10 and 50 μ M. These biofilms developed over 48 h at 37°C, as described in Materials and Methods, and were stained with a lipophilic fluorescent green dye (FM 1-43). Representative images from each flow channel are shown in Fig. 4A, along with 3D reconstructions from the z-stacks. Quantification of biomass and average thickness (calculated using Comstat 2) are shown in Fig. 4B and C. Biomass and thickness were substantially reduced at both concentrations of THD, indicating the inhibition of biofilm formation by THD is more pronounced under continuous flow than in static assays (Fig. 3B). Similar inhibition was observed for *A. baumannii* and *P. aeruginosa* when comparing bright-field microscopy images (Fig. S5).

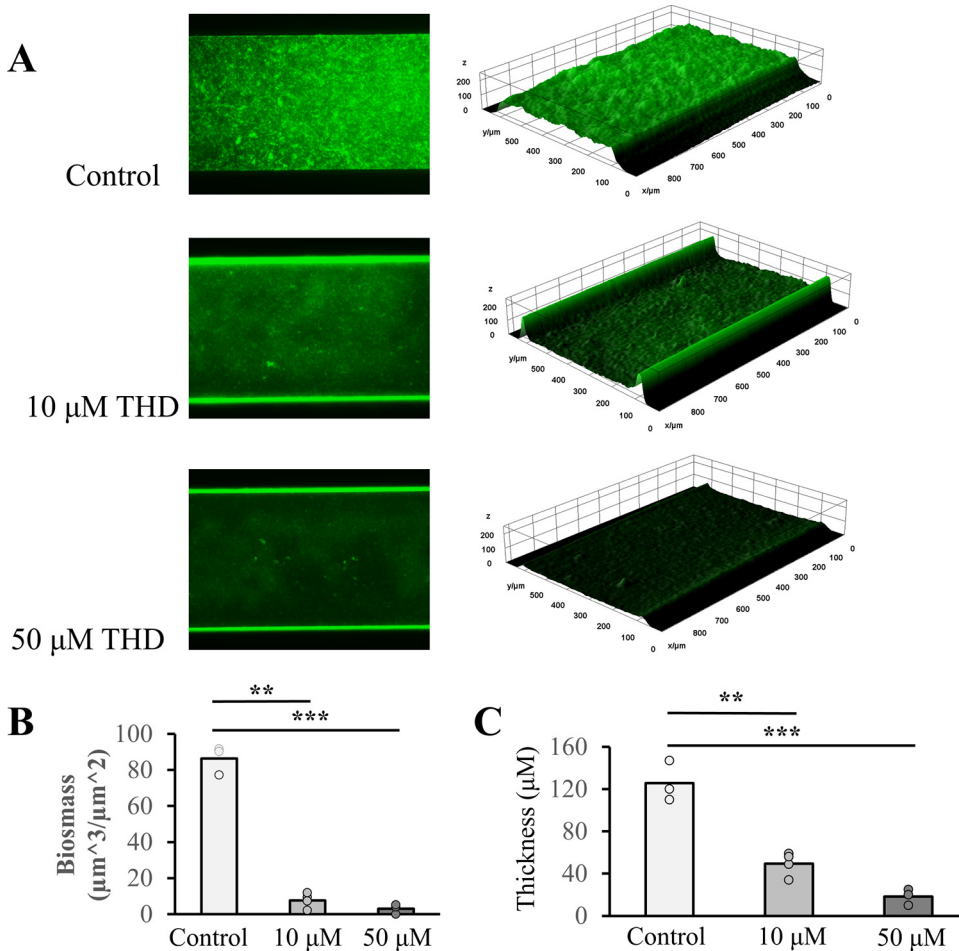


FIG 4 Continuous flow biofilms. (A) Representative *A. nosocomialis* M2 biofilms grown under continuous shear stress as a function of THD concentration. (B) Biomass as a function of THD concentration. (C) Biofilm thickness as a function of THD concentration. *, $P < 0.05$; **, $P < 0.01$; ***, $P < 0.001$; ns, not significant.

The inhibition of biofilm formation under continuous flow was much greater than either inhibition of twitching motility or static biofilm formation. At 50 μM THD, biofilms were reduced by over 90% in terms of biomass, comparable to those of the $\Delta pilA$ mutant, while measured twitching motility at that concentration was still within 50% of the wild type. The strong biofilm inhibition in this model supports the potential of phenothiazine compounds for use in combinatorial therapies against *Acinetobacter* infections.

Thiordazine shows activity against multiple *Acinetobacter* strains. Although *A. baumannii* is commonly thought to be the cause of most *Acinetobacter* infections (44–46), infections with other *Acinetobacter* species continue to be medically relevant (1, 47–50). Considerable variation also exists within *A. baumannii* (51, 52), including within the T4P system (11, 53). For these reasons, we measured the ability of phenothiazine treatment to reduce biofilm formation in a range of *Acinetobacter* species, both within the Acb complex (*A. baumannii* AB5075, *A. baumannii* ATCC 17978, and *A. nosocomialis* M2) and outside it (*A. radioresistens* FO-1 and *A. baylyi* ADP1). All Acb members are known pathogens, but they vary in their period of isolation; *A. baumannii* ATCC 17978 is a well-characterized lab strain (54), while AB5075 and *A. nosocomialis* M2 are more recent clinical isolates (16, 55). FO-1 and ADP1 are the type strains for their respective species and are known for their extremotolerance (56, 57) and natural transformability, respectively (58, 59). Importantly, all of these species and strains produce type IV pili, suggesting that an anti-T4P inhibitory compound should be effective against all of them.

Figure 5 shows the results of a static biofilm assay for each of the five strains with and without the addition of 50 μM THD (Fig. 5A), as well as a 16S dendrogram showing the

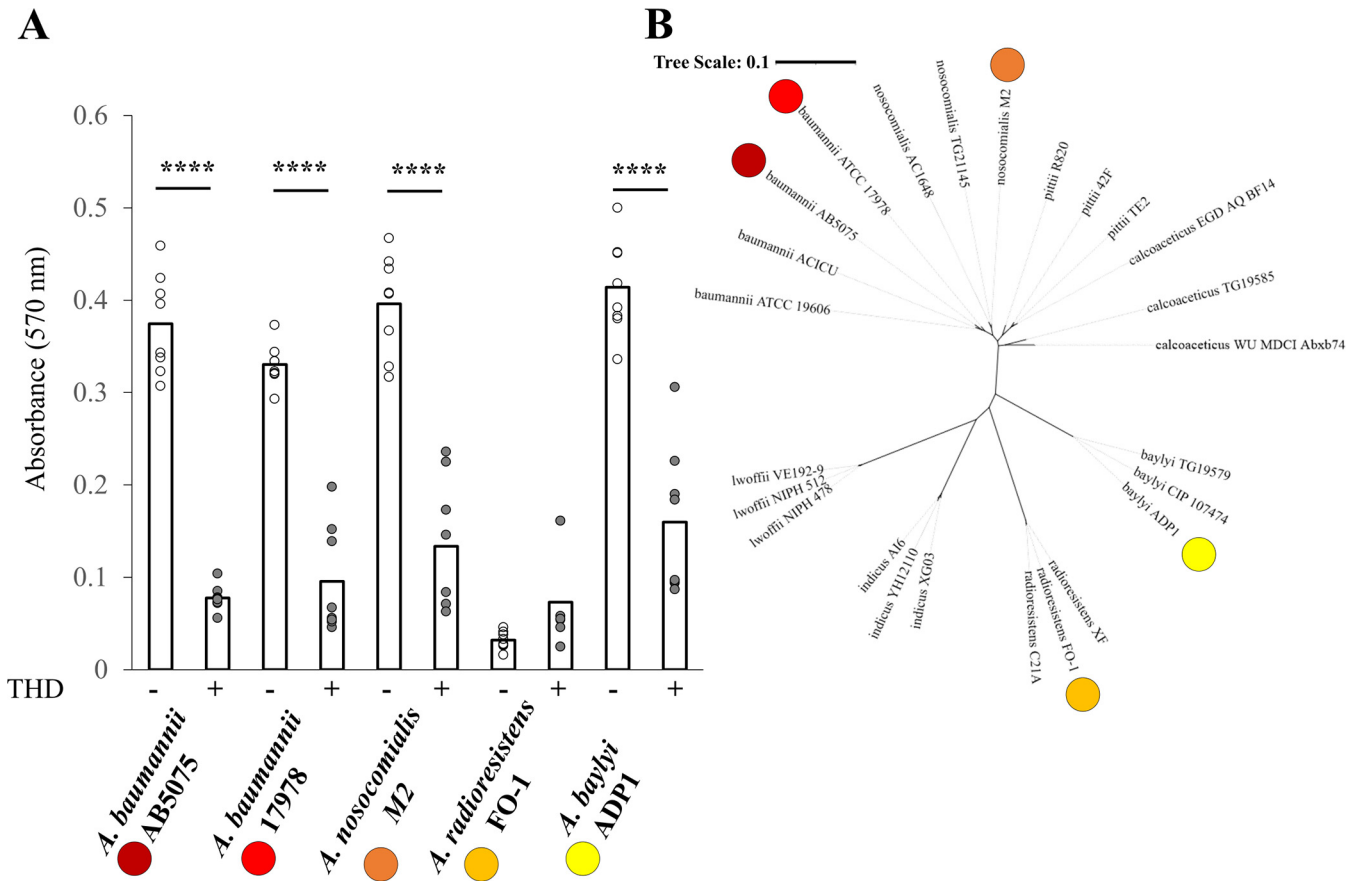


FIG 5 Broad THD activity against *Acinetobacter* biofilms. (A) Static biofilm assays for five *Acinetobacter* strains with and without 50 μ M thioridazine. (B) Dendrogram of selected *Acinetobacter* strains based on the 16S rRNA methyltransferase RsmB. Strains used in panel A assay are marked with corresponding colored dots. *, $P < 0.05$; **, $P < 0.01$; ***, $P < 0.001$; ****, $P < 0.0001$.

genetic relationships between these species and strains. Apart from *A. radioresistens* FO-1, which grew robustly under both conditions but formed very little biofilm, all strains showed significant reductions in biofilm as measured by crystal violet staining.

DISCUSSION

Although numerous physiological processes contribute to antimicrobial resistance, including drug efflux pumps and mutations to target gene products, bacterial biofilm formation remains a key factor because biofilms can persist through treatment even when isogenic planktonic cells are vulnerable (60–65). This resistance has been hypothesized to result from both the physical encapsulation and isolation from the environment (66) and the phenotypic differentiation within the biofilm making some cells metabolically inert or otherwise less vulnerable to antimicrobials (67). Biofilm inhibition or dispersal agents are an obvious solution but have been limited in their medical use by a variety of factors, including the wide variation within bacterial species which limits the utility of many specific agents (68).

Phenothiazines represent an intriguing opportunity as anti-biofilm agents because of their established activity against multiple bacteria taxa (25, 31, 34). The broad antimicrobial activity of phenothiazines, particularly thioridazine, is likely an integrated effect from numerous targets in bacterial cell membranes. However, data from our group and others suggest that inhibition of type IV pili and related filaments may be a common factor. Type IV pili are produced by a wide range of bacteria, including *N. meningitidis* (23, 69), *P. aeruginosa* (7, 19, 38, 70), and *Acinetobacter* spp. (11, 43), while *M. tuberculosis* and *S. aureus* produce structurally related tad/flp pili (71, 72) and competence (com) pili (73), respectively. Both T4P and com pili are known to bind DNA, while both T4P and extracellular DNA (eDNA) are known to be essential for bacterial biofilms in numerous species (8, 11, 37, 74–78). The results from

studies of mutants lacking DNA-binding subunits suggest that pilus/DNA interactions stabilize biofilms (79). Here, we report the activity of two phenothiazine compounds against *Acinetobacter* biofilm and twitching motility at concentrations that do not show substantial inhibition of growth. The simplest explanation for these results *in toto* is that THD and TFP inhibit *Acinetobacter* biofilm by targeting T4P.

To the extent that activity against helical filaments like T4P can explain biofilm inhibition, the mechanism by which phenothiazines inhibit T4P function is of general interest. Previously, Denis et al. found that TFP or THD reduced piliation in *N. meningitidis*, but not expression of *pilE* (the homologue of *Acinetobacter pilA*), suggesting that both compounds inhibit pilus biogenesis rather than the expression of pilus subunits (25). Our results are consistent with this hypothesis, as we observed defects in both retraction-dependent twitching motility (Fig. 2) and retraction-independent biofilm formation (Fig. 3 and 4).

Experimentally, multiple models of bacterial biofilm formation are commonly used, including horizontal (80) and vertical (11) models of static biofilm formation. Continuous flow bioreactors, including the BioFlux system used here, have advantages both in the constant removal of nonadherent cells and the application of shear stress to the extracellular matrix (42, 81). Despite extensive literature showing defects in biofilm formation for bacterial mutants of type IV pilus genes (78, 82, 83), this is the first study, to our knowledge, which has measured this defect in a continuous flow model (Fig. S4 in the supplemental material). Compared directly, the defect in biofilm formation induced by THD is more pronounced under continuous flow than in static assays, particularly at a lower concentration (10 μ M) (compare Fig. 3B with Fig. 4B and C). This difference is consistent with previous data showing greater differences in biofilm formation in continuous flow assays (5).

If the antimicrobial activity of phenothiazines stems, either wholly or partially, from a decrease in biofilm mediated by inhibition of pilus biogenesis, this could explain why the most dramatic results have been obtained through combined treatments in which phenothiazines potentiate the use of other antimicrobials (31, 33). Biofilm dispersal agents have been shown to potentiate other antimicrobials against numerous bacterial species (84).

Type IVa pilus systems like those found in *Acinetobacter*, *Pseudomonas*, and other *Moraxellaceae* species are involved in multiple potentially pathogenic processes, including host-cell adhesion, surface motility, horizontal gene transfer, and biofilm formation, leading to their moniker of “prokaryotic Swiss army knives” (82). This widespread activity makes them natural therapeutic targets and the use of anti-T4P compounds has precedent in *Acinetobacter*; Nait Chabane et al. found that Virstatin, a T4P-inhibitor, could reduce both motility and biofilm formation (54). The potential for phenothiazine use against *Acinetobacter* infections may depend on the strain and location of the infection. Results from several epidemiological studies suggest that *A. baumannii* lineages are preferentially associated with certain types of infections. Matsui et al. found that European clone II isolates made up 43% of lung infections but 0% of blood infections and only 2% of other infections (85), and Eijkelkamp et al. found that European clone II stains formed 70% more biofilm than other lineages (51). Vijayakumar et al. compared the biofilm formation capacity of lung and blood isolates and found that lung isolates formed more biofilm (approximately twice as much) on average (86). Differential roles for biofilm based on the infection site may explain why Wang et al. found no relationship between biofilm formation from clinical isolates and clinical outcomes in patients with bloodborne infections (bacteremia) (87). Taken together, these results suggest that biofilm dispersal agents (including phenothiazines) in *Acinetobacter* treatment may be best used for persistent lung infections, while bloodborne infections require other tools.

The broad activity observed here against biofilm formation in several *Acinetobacter* species (Fig. 5) is encouraging, particularly taken together with prior studies of distantly related bacterial taxa. However, we expect that phenothiazines likely have pleiotropic effects both against *Acinetobacter* and other genera. The cytotoxic activity we observed against *M. bovoculi* cannot be explained by activity against any function of T4P, which is not essential for growth in broth (and, in fact, is generally poorly expressed in liquid culture). In humans, phenothiazine compounds are known to have activity against a wide range of membrane receptors (88) and, based on the combination of effects observed here (both anti-piliation and cytotoxicity), we

expect that multiple bacterial membrane receptors are potential targets. Effective evaluation of specific activities, such as the inhibition of type IV pilus biogenesis, will require careful controls as well as specific assays (for example, twitching motility is specific for type IV pili, while many surface structures can contribute to general surface motility).

As the level of multidrug resistance in *Acinetobacter* infections increases, resistance is being encountered even to “last-resort” antibiotics such as colistin (89, 90). The development of combinatorial treatments which combine existing compounds approved for human use may be the most promising path forward for combating novel antimicrobial resistance as it develops. Several phenothiazine compounds have extensive histories of use in humans, including chlorpromazine, perphenazine, prochlorperazine, and promethazine, in addition to the two used in this study, thioridazine and trifluoperazine (26, 29). However, their use has been limited in some cases due to their toxicity, including ocular toxicity (91). Because courses of antibiotic treatment are generally short, the side effects of phenothiazine compounds may be less of a concern for their use as antimicrobials than for their use as anti-psychotics. The broad activity against biofilm formation by *Acinetobacter* species shown here for thioridazine suggests that phenothiazine compounds will be useful in combating *Acinetobacter* antimicrobial resistance where it is mediated by biofilm. These results, in combination with those from studies of other bacteria, suggest that similar results may be obtained for a range of bacterial species which utilize helical pili to form biofilm.

MATERIALS AND METHODS

Bacterial strains. *A. nosocomialis* wild type, $\Delta pilA$ mutant, and the complement have been described previously (16, 43). *A. baumannii* AB5075-UW was purchased from the University of Washington’s AB5075 mutant library (92). *P. aeruginosa* PAO1, *A. baylyi* ADP1, *A. baumannii* ATCC 17978, and *A. radioresistens* FO-1 were purchased from the American Type Culture collection (ATCC). *M. bovoculi* 58086 was provided by Dustin Loy’s group at the University of Nebraska-Lincoln.

Phenothiazine compounds. Thioridazine (also known as Novoridazine) and trifluoperazine (also known as Stelazine), purchased from Tokyo Chemical Industry Co., Ltd. (TCI) America, were dissolved in double-distilled water (ddH₂O) at stock concentrations of 10 mM and stored frozen in 1-mL aliquots at –20°C. Aliquots were thawed and added to bacterial growth medium (LB or MacConkey) at working concentrations of 10 to 50 μ M immediately before use. For solid media, THD or TFP was added to the agar after cooling to 50°C as the plates were poured and thoroughly mixed before the agar solidified.

Planktonic growth. Growth in liquid medium was measured by optical density at 600 nm using a Synergy H1 (BioTek Instruments) plate reader at 37°C in 96-well plates with MacConkey broth (Difco) (*A. nosocomialis* and *P. aeruginosa*) or brain heart infusion (BHI) broth (Remel) (*M. bovoculi*). Overnight cultures of each bacterial species were added at 1:10 and growth measured for at least 6 h with periodic shaking for equilibration (93).

Twitching motility. For all bacterial strains, bacteria were grown on solid medium (LB agar at 1.5%) overnight at 37°C. For measuring twitching motility, assay plates were made using MacConkey medium with 1.0% agar (previously found by our group to increase twitching in *Acinetobacter* species [11]). Multiple colonies were removed from a single plate grown overnight and inoculated into the assay plates by stabbing through the agar to the interface between the medium and the petri dish. Assay plates were incubated at 37°C for at least 48 h in sealed bags with moist paper towels (to control humidity for the duration of the assay). Twitching was measured by removing the agar medium from the petri dish and staining the bacteria adherent to the petri dish with 0.1% crystal violet in phosphate-buffered saline (PBS; 20 mM NaPO₄, 150 mM NaCl [pH 7.4]). After staining, petri dishes were washed with PBS to remove nonspecific crystal violet and twitching area was measured in two directions 90 degrees apart as described previously (11, 94). Total twitching area was measured as a fraction of the plate’s total area calculated from the radius of the plate in the image.

Static biofilm formation. Static biofilm formation was measured after growth in LB medium without added NaCl (5 g yeast extract and 10 g peptone per L). Next, 96-well plates were inoculated 1:20 with bacteria grown overnight at 37°C. Plates were then incubated at 37°C for 72 h, with liquid medium exchanged after 24 and 48 h. Wells were then washed 3 times with PBS, stained with 0.01% crystal violet for 10 min, and washed three more times with PBS. Crystal violet was dissolved in 30% acetic acid and measured (after dilution) by absorbance at 550 nm using a Synergy H1 plate reader (BioTek Instruments) (5). Similar results were obtained using MacConkey medium (Fig. S6).

Biofilm formation under continuous flow. Bacterial biofilms were grown in a 1:5 dilution of MacConkey medium, under continuous shear stress, in a BioFlux 200 (Fluxion Biosystems) over 48 h at a flow rate of 1 μ L/min. Progression was monitored using bright-field microscopy with an EVOS m5000 (Thermo Fisher). For imaging, biofilms were fluorescently stained for 5 min using FM 1-43 (Thermo Fisher), a green fluorescent lipophilic dye, at 4 mM in PBS, and washed using 50 μ L PBS (20 mM NaPO₄, 150 mM NaCl [pH 7.4]) at 5 μ L/min, similar to previous studies (79, 95). The resulting fluorescent bacterial biofilms were imaged using the EVOS m5000; z-stacks were taken, and the resulting 3D composite images were analyzed for biomass and thickness using Comstat 2 (96) and ImageJ (97).

Congo red/brilliant blue uptake. This assay was performed as described previously (41). Briefly, solid medium for these plates consisted of 15 g/L peptone, 10 g/L lactose, 1.5 g/L bile salts, 13.5 g/L agar, 40 mg/L Congo red, and 20 mg/L Coomassie brilliant blue. Bacterial suspensions were spotted in replicates

on multiple plates grown for 24 h at 37°C. The images were analyzed using ImageJ (97), with the intensity of the blue channel used to determine the density of dye for each colony.

Statistical analysis. All experiments included at least three technical replicates. Statistical analyses were performed using R for Windows 3.6.1; comparisons between groups used Student's one-tailed *t* test.

SUPPLEMENTAL MATERIAL

Supplemental material is available online only.

SUPPLEMENTAL FILE 1, PDF file, 0.9 MB.

ACKNOWLEDGMENTS

We would like to extend our appreciation to the Manoil group at the University of Washington, Dustin Loy (University of Nebraska-Lincoln) and Christian Harding (VaxNewMo) for strains used in this study.

This work was supported by National Institutes of Health grants K22-AI123467 (to K.H.P.) and P20-GM113126 (K.H.P. was a young investigator through the Nebraska Center for Integrated Biomolecular Communication).

The content is solely the responsibility of the authors and does not necessarily represent the official views of the National Institutes of Health.

N.V.: Investigation, Formal analysis, Writing – Original Draft. B.S.: Validation. Y.Y.: Investigation, Methodology. K.H.P.: Supervision, Funding acquisition, Writing – Review & Editing.

We declare that we have no known competing financial interests or personal relationships that could have appeared to influence the work reported in this paper.

REFERENCES

- Ejaz H, Qamar MU, Junaid K, Younas S, Taj Z, Bukhari SNA, Abdalla AE, Abosalif KOA, Ahmad N, Saleem Z, Salem EHM. 2022. The molecular detection of class B and class D carbapenemases in clinical strains of *Acinetobacter calcoaceticus-baumannii* complex: the high burden of antibiotic resistance and the co-existence of carbapenemase genes. *Antibiotics (Basel)* 11:1168. <https://doi.org/10.3390/antibiotics11091168>.
- CDC. 2019. Antibiotic resistance threats in the United States. CDC, Atlanta, GA.
- Mulani MS, Kamble EE, Kumkar SN, Tawre MS, Pardesi KR. 2019. Emerging strategies to combat ESKAPE pathogens in the era of antimicrobial resistance: a review. *Front Microbiol* 10:539. <https://doi.org/10.3389/fmicb.2019.00539>.
- Weiner LM, Webb AK, Limbago B, Dudeck MA, Patel J, Kallen AJ, Edwards JR, Sievert DM. 2016. Antimicrobial-resistant pathogens associated with healthcare-associated infections: summary of data reported to the National Healthcare Safety Network at the Centers for Disease Control and Prevention, 2011–2014. *Infect Control Hosp Epidemiol* 37:1288–1301. <https://doi.org/10.1017/ice.2016.174>.
- Kavanaugh JS, Flack CE, Lister J, Ricker EB, Ibberson CB, Jenul C, Moormeier DE, Delmain EA, Bayles KW, Horswill AR. 2019. Identification of extracellular DNA-binding proteins in the biofilm Matrix. *mBio* 10:e01137-19. <https://doi.org/10.1128/mBio.01137-19>.
- Moon KH, Weber BS, Feldman MF. 2017. Subinhibitory concentrations of trimethoprim and sulfamethoxazole prevent biofilm formation by *Acinetobacter baumannii* through inhibition of Csu pilus expression. *Antimicrob Agents Chemother* 61:e00778-17. <https://doi.org/10.1128/AAC.00778-17>.
- Gellatly SL, Hancock RE. 2013. *Pseudomonas aeruginosa*: new insights into pathogenesis and host defenses. *Pathog Dis* 67:159–173. <https://doi.org/10.1111/2049-632X.12033>.
- Maldarelli GA, Piepenbrink KH, Scott AJ, Freiberg JA, Song Y, Achermann Y, Ernst RK, Shirliff ME, Sundberg EJ, Donnenberg MS, von Rosenvinge EC. 2016. Type IV pili promote early biofilm formation by *Clostridium difficile*. *Pathog Dis* 74. <https://doi.org/10.1093/femspd/ftw061>.
- Hung C, Zhou Y, Pinkner JS, Dodson KW, Crowley JR, Heuser J, Chapman MR, Hadjifrangiskou M, Henderson JP, Hultgren SJ. 2013. *Escherichia coli* biofilms have an organized and complex extracellular matrix structure. *mBio* 4:e00645-13. <https://doi.org/10.1128/mBio.00645-13>.
- Bordeleau E, Purcell EB, Lafontaine DA, Fortier LC, Tamayo R, Burrus V. 2015. Cyclic di-GMP riboswitch-regulated type IV pili contribute to aggregation of *Clostridium difficile*. *J Bacteriol* 197:819–832. <https://doi.org/10.1128/JB.02340-14>.
- Ronish LA, Lillehoj E, Fields JK, Sundberg EJ, Piepenbrink KH. 2019. The structure of PilA from *Acinetobacter baumannii* AB5075 suggests a mechanism for functional specialization in *Acinetobacter* type IV pili. *J Biol Chem* 294: 218–230. <https://doi.org/10.1074/jbc.RA118.005814>.
- Piepenbrink KH. 2019. DNA uptake by type IV filaments. *Front Mol Biosci* 6:1. <https://doi.org/10.3389/fmolb.2019.00001>.
- Pellic V. 2008. Type IV pili: e pluribus unum? *Mol Microbiol* 68:827–837. <https://doi.org/10.1111/j.1365-2958.2008.06197.x>.
- Aas FE, Wolfgang M, Frye S, Dunham S, Løvold C, Koomey M. 2002. Competence for natural transformation in *Neisseria gonorrhoeae*: components of DNA binding and uptake linked to type IV pilus expression. *Mol Microbiol* 46:749–760. <https://doi.org/10.1046/j.1365-2958.2002.03193.x>.
- Antonova ES, Hammer BK. 2015. Genetics of natural competence in *Vibrio cholerae* and other *Vibrios*. *Microbiol Spectr* 3. <https://doi.org/10.1128/microbiolspec.VE-0010-2014>.
- Harding CM, Tracy EN, Carruthers MD, Rather PN, Actis LA, Munson RS. 2013. *Acinetobacter baumannii* strain M2 produces type IV pili which play a role in natural transformation and twitching motility but not surface-associated motility. *mBio* 4:e00360-13. <https://doi.org/10.1128/mBio.00360-13>.
- Allison TM, Conrad S, Castric P. 2015. The group I pilin glycan affects type IV pilus hydrophobicity and twitching motility in *Pseudomonas aeruginosa* 1244. *Microbiology (Reading)* 161:1780–1789. <https://doi.org/10.1099/mic.0.000128>.
- Bakkali M. 2013. Could DNA uptake be a side effect of bacterial adhesion and twitching motility? *Arch Microbiol* 195:279–289. <https://doi.org/10.1007/s00203-013-0870-1>.
- Bradley DE. 1980. A function of *Pseudomonas aeruginosa* PAO polar pili: twitching motility. *Can J Microbiol* 26:146–154. <https://doi.org/10.1139/m80-022>.
- Henrichsen J. 1983. Twitching motility. *Annu Rev Microbiol* 37:81–93. <https://doi.org/10.1146/annurev.mi.37.100183.000501>.
- Marathe R, Meel C, Schmidt NC, Dewenter L, Kurre R, Greune L, Schmidt MA, Müller MJ, Lipowsky R, Maier B, Klumpp S. 2014. Bacterial twitching motility is coordinated by a two-dimensional tug-of-war with directional memory. *Nat Commun* 5:3759. <https://doi.org/10.1038/ncomms4759>.
- Merz AJ, So M, Sheetz MP. 2000. Pilus retraction powers bacterial twitching motility. *Nature* 407:98–102. <https://doi.org/10.1038/35024105>.
- Barnier JP, Meyer J, Kolappan S, Bouzinba-Segard H, Gesbert G, Jamet A, Frapy E, Schonherr-Hellec S, Capel E, Virion Z, Dupuis M, Bille E, Morand P, Schmitt T, Bourdoulous S, Nassif X, Craig L, Coureuil M. 2021. The minor pilin PilV provides a conserved adhesion site throughout the antigenically variable meningococcal type IV pilus. *Proc Natl Acad Sci U S A* 118:e2109364118. <https://doi.org/10.1073/pnas.2109364118>.

24. Hélaïne S, Carbone E, Prouvensier L, Beretti JL, Nassif X, Pelicic V. 2005. PilX, a pilus-associated protein essential for bacterial aggregation, is a key to pilus-facilitated attachment of *Neisseria meningitidis* to human cells. *Mol Microbiol* 55:65–77. <https://doi.org/10.1111/j.1365-2958.2004.04372.x>.
25. Denis K, Le Bris M, Le Guennec L, Barnier JP, Faure C, Gouge A, Bouzinba-Segard H, Jamet A, Euphrasie D, Durel B, Barois N, Pelissier P, Morand PC, Coureuil M, Lafont F, Join-Lambert O, Nassif X, Bourdoulous S. 2019. Targeting Type IV pili as an antivirulence strategy against invasive meningococcal disease. *Nat Microbiol* 4:972–984. <https://doi.org/10.1038/s41564-019-0395-8>.
26. Hamilton RJ. 2020. Tarascon pocket pharmacopoeia: 2020 classic shirt-pocket ed, Jones & Bartlett Learning LLC, Burlington, MA.
27. Currihan M. 2021. The drug recognition guide, 2nd ed. Wiley-Blackwell, Hoboken, NJ.
28. Leucht S, Cipriani A, Spinelli L, Mavridis D, Orey D, Richter F, Samara M, Barbui C, Engel RR, Geddes JR, Kissling W, Stapf MP, Lassig B, Salanti G, Davis JM. 2013. Comparative efficacy and tolerability of 15 antipsychotic drugs in schizophrenia: a multiple-treatments meta-analysis. *Lancet* 382: 951–962. [https://doi.org/10.1016/S0140-6736\(13\)60733-3](https://doi.org/10.1016/S0140-6736(13)60733-3).
29. Jaszczyszyn A, Gąsiorowski K, Świątek P, Malinka W, Cieślak-Boczula K, Petrus J, Czarnik-Matusiewicz B. 2012. Chemical structure of phenothiazines and their biological activity. *Pharmacol Rep* 64:16–23. [https://doi.org/10.1016/s1734-1140\(12\)70726-0](https://doi.org/10.1016/s1734-1140(12)70726-0).
30. Ohlow MJ, Moosmann B. 2011. Phenothiazine: the seven lives of pharmacology's first lead structure. *Drug Discov Today* 16:119–131. <https://doi.org/10.1016/j.drudis.2011.01.001>.
31. Amaral L, Viveiros M. 2012. Why thioridazine in combination with antibiotics cures extensively drug-resistant *Mycobacterium tuberculosis* infections. *Int J Antimicrob Agents* 39:376–380. <https://doi.org/10.1016/j.ijantimicag.2012.01.012>.
32. Amaral L, Kristiansen JE, Viveiros M, Atouguia J. 2001. Activity of phenothiazines against antibiotic-resistant *Mycobacterium tuberculosis*: a review supporting further studies that may elucidate the potential use of thioridazine as anti-tuberculosis therapy. *J Antimicrob Chemother* 47:505–511. <https://doi.org/10.1093/jac/47.5.505>.
33. Thanacoody HK. 2007. Thioridazine: resurrection as an antimicrobial agent? *Br J Clin Pharmacol* 64:566–574. <https://doi.org/10.1111/j.1365-2125.2007.03021.x>.
34. Thorsing M, Klitgaard JK, Atilano ML, Skov MN, Kolmos HJ, Filipe SR, Kallipolitis BH. 2013. Thioridazine induces major changes in global gene expression and cell wall composition in methicillin-resistant *Staphylococcus aureus* USA300. *PLoS One* 8:e64518. <https://doi.org/10.1371/journal.pone.0064518>.
35. Kristiansen MM, Leandro C, Ordway D, Martins M, Viveiros M, Pacheco T, Kristiansen JE, Amaral L. 2003. Phenothiazines alter resistance of methicillin-resistant strains of *Staphylococcus aureus* (MRSA) to oxacillin *in vitro*. *Int J Antimicrob Agents* 22:250–253. [https://doi.org/10.1016/s0924-8579\(03\)00200-0](https://doi.org/10.1016/s0924-8579(03)00200-0).
36. Hu Y, He L, Tao X, Meng F, Zhang J. 2019. High DNA uptake capacity of international clone II *Acinetobacter baumannii* detected by a novel planktonic natural transformation assay. *Front Microbiol* 10:2165. <https://doi.org/10.3389/fmicb.2019.02165>.
37. Klausen M, Heydorn A, Ragas P, Lambertsens L, Aaes-Jorgensen A, Molin S, Tolker-Nielsen T. 2003. Biofilm formation by *Pseudomonas aeruginosa* wild type, flagella and type IV pili mutants. *Mol Microbiol* 48:1511–1524. <https://doi.org/10.1046/j.1365-2958.2003.03525.x>.
38. Barken KB, Pamp SJ, Yang L, Gjermansen M, Bertrand JJ, Klausen M, Givskov M, Whitchurch CB, Engel JN, Tolker-Nielsen T. 2008. Roles of type IV pili, flagellum-mediated motility and extracellular DNA in the formation of mature multicellular structures in *Pseudomonas aeruginosa* biofilms. *Environ Microbiol* 10: 2331–2343. <https://doi.org/10.1111/j.1462-2920.2008.01658.x>.
39. Chiang P, Burrows LL. 2003. Biofilm formation by hyperpiliated mutants of *Pseudomonas aeruginosa*. *J Bacteriol* 185:2374–2378. <https://doi.org/10.1128/JB.185.7.2374-2378.2003>.
40. Biswas I, Mettlach J. 2019. A simple static biofilm assay for *Acinetobacter baumannii*. *Methods Mol Biol* 1946:159–165. https://doi.org/10.1007/978-1-4939-9118-1_15.
41. Jones CJ, Wozniak DJ. 2017. Congo red stain identifies matrix overproduction and is an indirect measurement for c-di-GMP in many species of bacteria. *Methods Mol Biol* 1657:147–156. https://doi.org/10.1007/978-1-4939-7240-1_12.
42. Naudin B, Heins A, Pinhal S, De E, Nicol M. 2019. BioFlux 200 Microfluidic System to study *A. baumannii* biofilm formation in a dynamic mode of growth. *Methods Mol Biol* 1946:167–176. https://doi.org/10.1007/978-1-4939-9118-1_16.
43. Piepenbrink KH, Lillehoj E, Harding CM, Labonte JW, Zuo X, Rapp CA, Munson RS, Goldblum SE, Feldman MF, Gray JJ, Sundberg EJ. 2016. Structural diversity in the type IV pili of multidrug-resistant *Acinetobacter*. *J Biol Chem* 291: 22924–22935. <https://doi.org/10.1074/jbc.M116.751099>.
44. Dijkshoorn L, Nemec A, Seifert H. 2007. An increasing threat in hospitals: multidrug-resistant *Acinetobacter baumannii*. *Nat Rev Microbiol* 5:939–951. <https://doi.org/10.1038/nrmicro1789>.
45. Doi Y, Murray GL, Peleg AY. 2015. *Acinetobacter baumannii*: evolution of antimicrobial resistance-treatment options. *Semin Respir Crit Care Med* 36:85–98. <https://doi.org/10.1055/s-0034-1398388>.
46. Howard A, O'Donoghue M, Feeney A, Sleator RD. 2012. *Acinetobacter baumannii*: an emerging opportunistic pathogen. *Virulence* 3:243–250. <https://doi.org/10.4161/viru.19700>.
47. Harding CM, Kinsella RL, Palmer LD, Skaar EP, Feldman MF. 2016. Medically relevant *Acinetobacter* species require a type II secretion system and specific membrane-associated chaperones for the export of multiple substrates and full virulence. *PLoS Pathog* 12:e1005391. <https://doi.org/10.1371/journal.ppat.1005391>.
48. Harding CM, Nasr MA, Kinsella RL, Scott NE, Foster LJ, Weber BS, Fiester SE, Actis LA, Tracy EN, Munson RS Jr, Feldman MF. 2015. *Acinetobacter* strains carry two functional oligosaccharyltransferases, one devoted exclusively to type IV pilin, and the other one dedicated to O-glycosylation of multiple proteins. *Mol Microbiol* 96:1023–1041. <https://doi.org/10.1111/mmi.12986>.
49. Cosgaya C, Marí-Almirall M, Van Assche A, Fernández-Orth D, Mosqueda N, Telli M, Huys G, Higgins PG, Seifert H, Lievens B, Roca I, Vila J. 2016. *Acinetobacter dijkshoorniae* sp. nov., a member of the *Acinetobacter calcoaceticus-Acinetobacter baumannii* complex mainly recovered from clinical samples in different countries. *Int J Syst Evol Microbiol* 66:4105–4111. <https://doi.org/10.1099/ijsem.0.001318>.
50. Nemec A, Krizova L, Maixnerova M, Sedo O, Brisse S, Higgins PG. 2015. *Acinetobacter seifertii* sp. nov., a member of the *Acinetobacter calcoaceticus-Acinetobacter baumannii* complex isolated from human clinical specimens. *Int J Syst Evol Microbiol* 65:934–942. <https://doi.org/10.1099/ijs.0.000043>.
51. Eijkelkamp BA, Stroehrer UH, Hassan KA, Papadimitriou MS, Paulsen IT, Brown MH. 2011. Adherence and motility characteristics of clinical *Acinetobacter baumannii* isolates. *FEMS Microbiol Lett* 323:44–51. <https://doi.org/10.1111/j.1574-6968.2011.02362.x>.
52. Zarrilli R, Pournaras S, Giannouli M, Tsakris A. 2013. Global evolution of multidrug-resistant *Acinetobacter baumannii* clonal lineages. *Int J Antimicrob Agents* 41:11–19. <https://doi.org/10.1016/j.ijantimicag.2012.09.008>.
53. Piepenbrink KH, Sundberg EJ. 2016. Motility and adhesion through type IV pili in Gram-positive bacteria. *Biochem Soc Trans* 44:1659–1666. <https://doi.org/10.1042/BST20160221>.
54. Nait Chabane Y, Mlouka MB, Alexandre S, Nicol M, Marti S, Pestel-Caron M, Vila J, Jouenne T, De E. 2014. Virastatin inhibits biofilm formation and motility of *Acinetobacter baumannii*. *BMC Microbiol* 14:62. <https://doi.org/10.1186/1471-2180-14-62>.
55. Jacobs AC, Thompson MG, Black CC, Kessler JL, Clark LP, McQueary CN, Gancz HY, Corey BW, Moon JK, Si Y, Owen MT, Hallock JD, Kwak YI, Summers A, Li CZ, Rasko DA, Penwell WF, Honnold CL, Wise MC, Waterman PE, Lesho EP, Stewart RL, Actis LA, Palys TJ, Craft DW, Zurawski DV. 2014. AB5075, a highly virulent isolate of *Acinetobacter baumannii*, as a model strain for the evaluation of pathogenesis and antimicrobial treatments. *mBio* 5:e01076-14. <https://doi.org/10.1128/mBio.01076-14>.
56. Mazzoli R, Fattori P, Lamberti C, Giuffrida MG, Zapponi M, Giunta C, Pessione E. 2011. High isoelectric point sub-proteome analysis of *Acinetobacter radioresistens* S13 reveals envelope stress responses induced by aromatic compounds. *Mol Biosyst* 7:598–607. <https://doi.org/10.1039/c0mb00112k>.
57. McCoy KB, Derecho I, Wong T, Tran HM, Huynh TD, La Duc MT, Venkateswaran K, Mogul R. 2012. Insights into the extremotolerance of *Acinetobacter radioresistens* 50v1, a Gram-negative bacterium isolated from the Mars Odyssey spacecraft. *Astrobiology* 12:854–862. <https://doi.org/10.1089/ast.2012.0835>.
58. Leong CG, Bloomfield RA, Boyd CA, Dornbusch AJ, Lieber L, Liu F, Owen A, Slay E, Lang KM, Lostroh CP. 2017. The role of core and accessory type IV pilus genes in natural transformation and twitching motility in the bacterium *Acinetobacter baylyi*. *PLoS One* 12:e0182139. <https://doi.org/10.1371/journal.pone.0182139>.
59. Hulter N, Sorum V, Borch-Pedersen K, Liljegren MM, Utnes AL, Primicerio R, Harms K, Johnsen PJ. 2017. Costs and benefits of natural transformation in *Acinetobacter baylyi*. *BMC Microbiol* 17:34. <https://doi.org/10.1186/s12866-017-0953-2>.
60. Kostakioti M, Hadjifrangiskou M, Hultgren SJ. 2013. Bacterial biofilms: development, dispersal, and therapeutic strategies in the dawn of the post-antibiotic era. *Cold Spring Harb Perspect Med* 3:a010306. <https://doi.org/10.1101/cshperspect.a010306>.
61. Yang J, Yun S, Park W. 2023. Blue light sensing BIsA-mediated modulation of meropenem resistance and biofilm formation in *Acinetobacter baumannii*. *Msystems* 8:e0089722. <https://doi.org/10.1128/msystems.00897-22>.

62. Tao Q, Wu Q, Zhang Z, Liu J, Tian C, Huang Z, Malakar PK, Pan Y, Zhao Y. 2022. Meta-analysis for the global prevalence of foodborne pathogens exhibiting antibiotic resistance and biofilm formation. *Front Microbiol* 13: 906490. <https://doi.org/10.3389/fmicb.2022.906490>.
63. Sparbrod M, Gager Y, Koehler AK, Jentsch H, Stingu CS. 2022. Relationship between phenotypic and genotypic resistance of subgingival biofilm samples in patients with periodontitis. *Antibiotics (Basel)* 12:68. <https://doi.org/10.3390/antibiotics12010068>.
64. Li P, Yu M, Ke X, Gong X, Li Z, Xing X. 2022. Cytocompatible amphiphatic carbon quantum dots as potent membrane-active antibacterial agents with low drug resistance and effective inhibition of biofilm formation. *ACS Appl Bio Mater* 5:3290–3299. <https://doi.org/10.1021/acsbm.2c00292>.
65. Dodson TA, Carlson EA, Wamer NC, Morse CN, Gadiant JN, Prestwich EG. 2022. Characterization of distinct biofilm cell subpopulations and implications in quorum sensing and antibiotic resistance. *mBio* 13:e0019122. <https://doi.org/10.1128/mbio.00191-22>.
66. Fey PD, Olson ME. 2010. Current concepts in biofilm formation of *Staphylococcus epidermidis*. *Future Microbiol* 5:917–933. <https://doi.org/10.2217/fmb.10.56>.
67. Muranaka LS, Takita MA, Olivato JC, Kishi LT, de Souza AA. 2012. Global expression profile of biofilm resistance to antimicrobial compounds in the plant-pathogenic bacterium *Xylella fastidiosa* reveals evidence of persister cells. *J Bacteriol* 194:4561–4569. <https://doi.org/10.1128/JB.00436-12>.
68. Verderosa AD, Totsika M, Fairfull-Smith KE. 2019. Bacterial biofilm eradication agents: a current review. *Front Chem* 7:824. <https://doi.org/10.3389/fchem.2019.00824>.
69. Aas FE, Winther-Larsen HC, Wolfgang M, Frye S, Løvold C, Roos N, van Putten JP, Kooimey M. 2007. Substitutions in the N-terminal alpha helical spine of *Neisseria gonorrhoeae* pilin affect type IV pilus assembly, dynamics and associated functions. *Mol Microbiol* 63:69–85. <https://doi.org/10.1111/j.1365-2958.2006.05482.x>.
70. Craig L, Pique ME, Tainer JA. 2004. Type IV pilus structure and bacterial pathogenicity. *Nat Rev Microbiol* 2:363–378. <https://doi.org/10.1038/nrmicro885>.
71. Alteri CJ, Xicohtencatl-Cortes J, Hess S, Caballero-Olin G, Giron JA, Friedman RL. 2007. *Mycobacterium tuberculosis* produces pili during human infection. *Proc Natl Acad Sci U S A* 104:5145–5150. <https://doi.org/10.1073/pnas.0602304104>.
72. Alteri CJ, Rios-Sarabia N, De la Cruz MA, González-Y-Merchand JA, Soria-Bustos J, Maldonado-Bernal C, Cedillo ML, Yáñez-Santos JA, Martínez-Laguna Y, Torres J, Friedman RL, Girón JA, Ares MA. 2022. The Flp type IV pilus operon of *Mycobacterium tuberculosis* is expressed upon interaction with macrophages and alveolar epithelial cells. *Front Cell Infect Microbiol* 12:916247. <https://doi.org/10.3389/fcimb.2022.916247>.
73. Cordero M, García-Fernández J, Acosta IC, Yepes A, Avendano-Ortiz J, Lisowski C, Oesterreich B, Ohlsen K, Lopez-Collazo E, Förstner KU, Eulalio A, Lopez D. 2022. The induction of natural competence adapts staphylococcal metabolism to infection. *Nat Commun* 13:1525. <https://doi.org/10.1038/s41467-022-29206-7>.
74. Purcell EB, McKee RW, Bordeleau E, Burrus V, Tamayo R. 2016. Regulation of type IV pili contributes to surface behaviors of historical and epidemic strains of *Clostridium difficile*. *J Bacteriol* 198:565–577. <https://doi.org/10.1128/JB.00816-15>.
75. Okshevsky M, Regina VR, Meyer RL. 2015. Extracellular DNA as a target for biofilm control. *Curr Opin Biotechnol* 33:73–80. <https://doi.org/10.1016/j.copbio.2014.12.002>.
76. Schlafer S, Meyer RL, Dige I, Regina VR. 2017. Extracellular DNA contributes to dental biofilm stability. *Caries Res* 51:436–442. <https://doi.org/10.1159/000477447>.
77. Whitchurch CB, Tolker-Nielsen T, Ragas PC, Mattick JS. 2002. Extracellular DNA required for bacterial biofilm formation. *Science* 295:1487. <https://doi.org/10.1126/science.295.5559.1487>.
78. Giltner CL, Nguyen Y, Burrows LL. 2012. Type IV pilin proteins: versatile molecular modules. *Microbiol Mol Biol Rev* 76:740–772. <https://doi.org/10.1128/MMBR.00035-12>.
79. Ronish LA, Sidner B, Yu Y, Piepenbrink KH. 2022. Recognition of extracellular DNA by type IV pili promotes biofilm formation by *Clostridioides difficile*. *J Biol Chem* 298:102449. <https://doi.org/10.1016/j.jbc.2022.102449>.
80. Weiss-Muszkat M, Shakh D, Zhou Y, Pinto R, Belausov E, Chapman MR, Sela S. 2010. Biofilm formation by and multicellular behavior of *Escherichia coli* O55:H7, an atypical enteropathogenic strain. *Appl Environ Microbiol* 76: 1545–1554. <https://doi.org/10.1128/AEM.01395-09>.
81. Goeres DM, Loetterle LR, Hamilton MA, Murga R, Kirby DW, Donlan RM. 2005. Statistical assessment of a laboratory method for growing biofilms. *Microbiology (Reading)* 151:757–762. <https://doi.org/10.1099/mic.0.27709-0>.
82. Berry JL, Pelicic V. 2015. Exceptionally wide-spread nanomachines composed of type IV pilins: the prokaryotic Swiss army knives. *FEMS Microbiol Rev* 39:134–154. <https://doi.org/10.1093/femsre/fuu001>.
83. Craig L, Li J. 2008. Type IV pili: paradoxes in form and function. *Curr Opin Struct Biol* 18:267–277. <https://doi.org/10.1016/j.sbi.2007.12.009>.
84. Fleming D, Rumbaugh K. 2018. The consequences of biofilm dispersal on the host. *Sci Rep* 8:10738. <https://doi.org/10.1038/s41598-018-29121-2>.
85. Matsui M, Suzuki M, Suzuki M, Yatsuyanagi J, Watahiki M, Hiraki Y, Kawano F, Tsutsui A, Shibayama K, Suzuki S. 2018. Distribution and molecular characterization of *Acinetobacter baumannii* international clone II lineage in Japan. *Antimicrob Agents Chemother* 62:e02190-17. <https://doi.org/10.1128/AAC.02190-17>.
86. Vijayakumar S, Rajenderan S, Laishram S, Anandan S, Balaji V, Biswas I. 2016. Biofilm formation and motility depend on the nature of the *Acinetobacter baumannii* clinical isolates. *Front Public Health* 4:105. <https://doi.org/10.3389/fpubh.2016.00105>.
87. Wang YC, Huang TW, Yang YS, Kuo SC, Chen CT, Liu CP, Liu YM, Chen TL, Chang FY, Wu SH, How CK, Lee YT. 2018. Biofilm formation is not associated with worse outcome in *Acinetobacter baumannii* bacteraemic pneumonia. *Sci Rep* 8:7289. <https://doi.org/10.1038/s41598-018-25661-9>.
88. Falkai P, Vogeley K. 2000. The chances of new atypical substances. [In German.] *Fortschr Neurol Psychiatr* 68 Suppl 1:S32–S37.
89. Li J, Rayner CR, Nation RL, Owen RJ, Spelman D, Tan KE, Liolios L. 2006. Heteroresistance to colistin in multidrug-resistant *Acinetobacter baumannii*. *Antimicrob Agents Chemother* 50:2946–2950. <https://doi.org/10.1128/AAC.00103-06>.
90. Qureshi ZA, Hittle LE, O'Hara JA, Rivera JJ, Syed A, Shields RK, Pasculle AW, Ernst RK, Doi Y. 2015. Colistin-resistant *Acinetobacter baumannii*: beyond carbapenem resistance. *Clin Infect Dis* 60:1295–1303. <https://doi.org/10.1093/cid/civ048>.
91. Soms CJ, Greene N, Render JA, Aleo MD, Fortner JH, Dykens JA, Phillips G. 2009. A current practice for predicting ocular toxicity of systemically delivered drugs. *Cutan Ocul Toxicol* 28:1–18. <https://doi.org/10.1080/15569520802618585>.
92. Gallagher LA, Ramage E, Weiss EJ, Radey M, Hayden HS, Held KG, Huse HK, Zurawski DV, Brittnacher MJ, Manoil C. 2015. Resources for genetic and genomic analysis of emerging pathogen *Acinetobacter baumannii*. *J Bacteriol* 197:2027–2035. <https://doi.org/10.1128/JB.00131-15>.
93. Stevenson K, McVey AF, Clark IBN, Swain PS, Pilizota T. 2016. General calibration of microbial growth in microplate readers. *Sci Rep* 6:38828. <https://doi.org/10.1038/srep38828>.
94. Biswas I, Machen A, Mettlach J. 2019. *In vitro* motility assays for *Acinetobacter* species. *Methods Mol Biol* 1946:177–187. https://doi.org/10.1007/978-1-4939-9118-1_17.
95. Houot L, Watnick PI. 2008. A novel role for enzyme I of the *Vibrio cholerae* phosphoenolpyruvate phosphotransferase system in regulation of growth in a biofilm. *J Bacteriol* 190:311–320. <https://doi.org/10.1128/JB.01410-07>.
96. Heydorn A, Nielsen AT, Hentzer M, Sternberg C, Givskov M, Ersbøll BK, Molin S. 2000. Quantification of biofilm structures by the novel computer program COMSTAT. *Microbiology* 146:2395–2407. <https://doi.org/10.1099/00221287-146-10-2395>.
97. Schmid B, Schindelin J, Cardona A, Longair M, Heisenberg M. 2010. A high-level 3D visualization API for Java and ImageJ. *BMC Bioinformatics* 11:274. <https://doi.org/10.1186/1471-2105-11-274>.